ACS OMEGA

Article

http://pubs.acs.org/journal/acsodf

Thermal Conductivity of Diamond/SiC Nano-Polycrystalline Composites and Phonon Scattering at Interfaces

Huicong Dong,[†] Bin Wen,*[,†] Yuwen Zhang,[‡] and Roderick Melnik[§]

[†]State Key Laboratory of Metastable Materials Science and Technology, Yanshan University, Qinhuangdao 066004, China

[‡]Department of Mechanical and Aerospace Engineering, University of Missouri—Columbia, Columbia, Missouri 65211, United States

[§]The MS2Discovery Interdisciplinary Research Institute, Wilfrid Laurier University, 75 University Avenue West, Waterloo, Ontario N2L 3C5, Canada

S *Supporting Information*

ABSTRACT: To compare the thermal properties of heterogeneous and homogeneous interfaces, polycrystalline composites are proposed. Thermal properties of heterogeneous and homogeneous interfaces in the composites are investigated using molecular dynamics simulations. The results indicate that when the inflow of heat arises from the same material, phonon scattering at heterogeneous interfaces is stronger than that at homogeneous interfaces. The phonon wave packet simulations indicate that the stronger phonon scattering at heterogeneous interfaces is caused by the combined actions of transmission coefficients and transmission time.

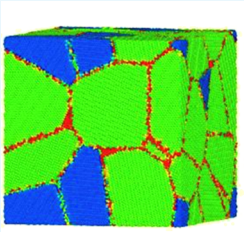

Diamond/SiC polycrystalline composites

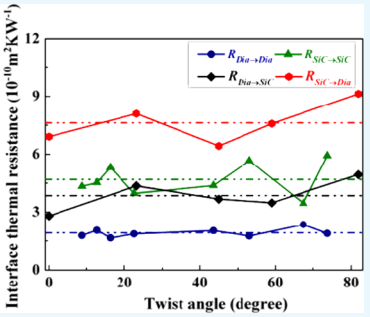

INTRODUCTION

Thermal conductivity of polycrystalline materials is of great interest because of its wide applications in many fields such as thermal barrier coatings,[1] bioMEMs,[2] and micro-/nano-electro-mechanical devices.[3] It is well-known that a large number of grain boundaries exist in polycrystalline materials,[4] thus leading to a large increase in their thermal resistance when compared with that of their corresponding single crystal.[5]

The thermal resistance of polycrystalline materials can be considered as a series of connections between intragranular and intergranular thermal resistances.[6] The intragranular thermal resistance of polycrystalline materials is determined by the thermal resistance and grain size of the bulk materials,[6] whereas the intergranular thermal resistance is determined by the characters of the grain boundaries.[7] A previous study on the adjustment of polycrystalline material thermal resistance was conducted mainly to change its grain size; hence, it is natural to imagine that adjusting the grain boundaries' characters may become another new way to adjust the thermal resistance of polycrystalline materials. The grain boundary formed by different phases, which is named heterogeneous interface, has been widely studied in experiments[8−10] and in simulations.[11,12] Results indicate that strong phonon scattering can be induced by heterogeneous interfaces.[8−12] Because of the asymmetry and lattice mismatch[13] of the heterogeneous interface, it probably induces stronger phonon scattering compared with the grain boundary formed by the same phase, which is named homogeneous interface.

To verify this hypothesis and study the effect of heterogeneous and homogeneous interfaces on the thermal conductivity of polycrystalline materials, polycrystalline composites are proposed, and the thermal properties of heterogeneous and homogeneous interfaces are studied in this work. Our simulated results demonstrate that when the inflow of heat arises from the same material, phonon scattering at heterogeneous interfaces is stronger than that at homogeneous interfaces because of the combined actions of energy transmission coefficients and transmission time.

RESULTS AND DISCUSSION

To study the thermal properties of heterogeneous and homogeneous interfaces, diamond/SiC polycrystalline composites have been proposed as a prototype in this work. Figure S1 shows a typical model of the diamond/SiC polycrystalline composites with periodic boundary conditions in three directions. As can be clearly seen in Figure S1, the structure of the polycrystalline composite is divided into three parts: the green parts are the SiC phase, the blue parts are the diamond phase, and the others are grain boundaries. The thermal conductivity of the composites with a grain size of 2 nm is calculated using nonequilibrium molecular dynamics (NEMD) simulations, and the results are plotted in Figure 1a. It can be seen that our simulated thermal conductivity of polycrystalline SiC and diamond agrees well with previously reported values,[6,14] indicating the reliability of NEMD simulation parameters used in our work. As the SiC volume fraction

Received: April 19, 2017
Accepted: May 10, 2017
Published: May 26, 2017

DOI: 10.1021/acsomega.7b00476
ACS Omega 2017, 2, 2344−2350

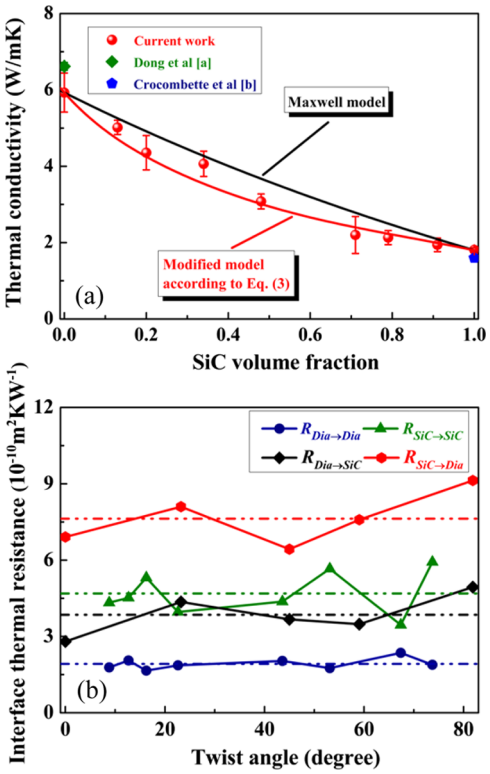

Figure 1. Thermal transmission properties in diamond/SiC polycrystalline composites. (a) Variation of thermal conductivity for diamond/SiC polycrystalline composites; the grain size is 2 nm, and the SiC volume fraction ranges from 0 to 100%. [a] refers to ref 5 and [b] refers to ref 13. (b) Thermal resistances for (001) heterogeneous and homogeneous interfaces with different twist angles. $R_{Dia\to SiC}$ and $R_{SiC\to Dia}$ are the thermal resistances of diamond/SiC heterogeneous interfaces when the heat flux transmits from diamond to SiC and in the opposite direction, respectively. $R_{Dia\to Dia}$ and $R_{SiC\to SiC}$ are the thermal resistances for diamond/diamond and SiC/SiC homogeneous interfaces, respectively.

increases, the thermal conductivity of the composites decreases. Here, a Maxwell model,[15] which is the most popular model to describe the thermal conductivity of composites with a spherical shape filler particle, is also applied to express the thermal conductivity of diamond/SiC polycrystalline composites. It has been demonstrated that the only defect of the Maxwell model is that it disregards the thermal resistance generated at the matrix and at the dispersed phase, and hence, it always overestimates the thermal conductivity of the composites. Assuming that polycrystalline diamond is the matrix phase and polycrystalline SiC is the dispersed phase, the thermal conductivity K of the diamond/SiC polycrystalline composite can be obtained by

$$K = K_{Dia}\cdot\left[\frac{2P_{SiC}\left(\frac{K_{Dia}}{K_{SiC}}-1\right)+\left(\frac{K_{Dia}}{K_{SiC}}+2\right)}{P_{SiC}\left(1-\frac{K_{Dia}}{K_{SiC}}\right)+\left(\frac{K_{Dia}}{K_{SiC}}+2\right)}\right] \quad (1)$$

where P_{SiC} is the volume fraction of polycrystalline SiC in composites and K_{Dia} and K_{SiC} are the thermal conductivities of polycrystalline diamond and SiC with a grain size of 2 nm, respectively. By comparing the thermal conductivity of diamond/SiC polycrystalline composites using NEMD simulation with the Maxwell model, it can be observed that the Maxwell model overestimates the thermal conductivity of the polycrystalline composites. On the basis of eq 1, the thermal conductivity of the polycrystalline composites is calculated by combining the thermal conductivities of polycrystalline diamond and SiC. According to ref 6, the factors that affect the thermal conductivity of polycrystalline materials are grain boundaries (diamond/diamond interfaces for polycrystalline diamond and SiC/SiC interfaces for polycrystalline SiC) and size effect. Thus, in the calculation of the thermal conductivity of the composites according to eq 1, although the effect of homogeneous interfaces (diamond/diamond interfaces and SiC/SiC interfaces) and the size effect on polycrystalline composites have been considered, the thermal resistance generated at the matrix (polycrystalline diamond) and at the dispersed phase (polycrystalline SiC) has been disregarded. Therefore, it can be deduced that the overestimation of thermal conductivity by the Maxwell model for diamond/SiC polycrystalline composites may be caused by the larger thermal resistance of the heterogeneous interface than that of the homogeneous interface.

To verify the deduction and study the different effects of heterogeneous and homogeneous interfaces on the thermal conductivity of diamond/SiC polycrystalline composites, thermal resistances of (001) heterogeneous (diamond/SiC) and homogeneous (diamond/diamond, SiC/SiC) interfaces with different twist angles were simulated. The lengths of the simulation cells used for the thermal resistance calculation are all 40 nm, and the effect of heat direction on the heterogeneous interface thermal resistance is taken into account. The calculated results are summarized in Figure 1b, and it can be seen that the thermal resistance of heterogeneous and homogeneous interfaces varies with different twist angles. The mean values of heterogeneous interface thermal resistance when heat flux transmits from diamond to SiC, $R_{Dia\to SiC}$, and in the opposite direction, $R_{SiC\to Dia}$, are 3.85×10^{-10} and 7.63×10^{-10} m^2 K/W, respectively. For homogeneous interfaces, the mean values of thermal resistance for diamond/diamond interfaces, $R_{Dia\to Dia}$, and SiC/SiC interfaces, $R_{SiC\to SiC}$, are approximately 1.92×10^{-10} and 4.69×10^{-10} m^2 K/W, respectively; these values are consistent with the previous simulated results.[6,14] By comparing the thermal resistances of heterogeneous and homogeneous interfaces, it can be found that the mean value of $R_{Dia\to SiC}$ is larger than that of $R_{Dia\to Dia}$, and $R_{SiC\to Dia}$ is larger than $R_{SiC\to SiC}$. Thus, it can be concluded that when the inflow of heat arises from the same material, phonon scattering at heterogeneous interfaces is stronger than that at homogeneous interfaces, confirming our deduction above. The strong phonon scattering at the heterogeneous interfaces has also been verified in many other systems experimentally.[8−10] Moreover, it can also be observed in Figure 1b that $R_{SiC\to Dia}$ is larger than $R_{Dia\to SiC}$, indicating the thermal rectification at heterogeneous interfaces, which has also been observed in other systems.[16,17] It has been reported that the rectification is caused by different thermal conductivities of materials on the two sides of the heterogeneous interface.[17]

By combining the calculated D-values between the heterogeneous and homogeneous interface thermal resistances and the Maxwell model, the thermal conductivity of diamond/SiC composites has been recalculated in a modified model, which is expressed by the following expression

$$\frac{1}{K} = \frac{1}{K_{Maxwell}} + \frac{\Delta R_K}{d}P \quad (2)$$

DOI: 10.1021/acsomega.7b00476
ACS Omega 2017, 2, 2344−2350

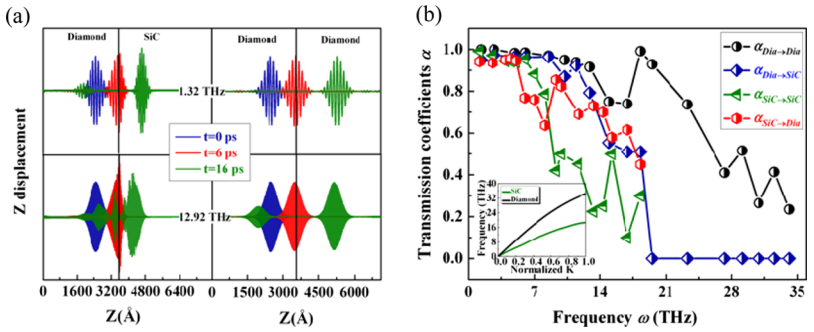

Figure 2. PWP simulations on heterogeneous and homogeneous interfaces. (a) Snapshots of the Z displacement of atoms for the wave packet with frequencies of 1.32 and 12.92 THz. The wave packet arises from diamond, and it scatters at (001) diamond/SiC (twist angle is 0°) and diamond/diamond (twist angle is 53.13°) interfaces separately. The vertical black line at Z = 3556 Å indicates the location of the interface. (b) Frequency-dependent energy transmission coefficients for heterogeneous and homogeneous interfaces. $\alpha_{Dia\rightarrow SiC}$ and $\alpha_{SiC\rightarrow Dia}$ are the transmission coefficients for (001) diamond/SiC interfaces (twist angle is 0°) when the wave packet transmits from diamond to SiC and in the opposite direction, respectively. $\alpha_{Dia\rightarrow Dia}$ and $\alpha_{SiC\rightarrow SiC}$ are the transmission coefficients for (001) diamond/diamond and SiC/SiC interfaces (twist angle is 53.13°), respectively. Inset: Comparison of LA phonon dispersion curves between diamond and SiC single crystals.

where $K_{Maxwell}$ is the thermal conductivity of the composites in the Maxwell model, ΔR_K is the D-value between the heterogeneous and homogeneous interface thermal resistances when the inflow of heat arises from the same material, d is the grain size, and P is the heterogeneous interface fraction that is calculated based on the probability theory, and it is a parameter related to the SiC volume fraction.

It is well-known that three kinds of interfaces in diamond/SiC polycrystalline composites exist, namely, diamond/diamond, SiC/SiC, and diamond/SiC interfaces. According to the probability theory, the fraction of diamond/diamond interfaces is $(1 - P_{SiC})^2$, the fraction of SiC/SiC interfaces is P_{SiC}^2, and the fraction of diamond/SiC interfaces is $2P_{SiC}(1 - P_{SiC})$. Considering the rectification of heterogeneous interfaces, diamond/SiC interfaces are divided into two kinds: One kind is the interface when the inflow of heat arises from diamond, assuming that the fraction of this kind of interface in the total heterogeneous interfaces equals the fraction of diamond/diamond interfaces in the total homogeneous interfaces$(1 - P_{SiC})^2/[P_{SiC}^2 + (1 - P_{SiC})^2]$; thus, the final fraction of this kind of interface in the total interfaces is $2P_{SiC}(1 - P_{SiC})^3/[P_{SiC}^2 + (1 - P_{SiC})^2]$. The other kind is the interface when the inflow of heat arises from SiC; in the same way, the final fraction of this kind of interface in the total interfaces can be obtained as $2P_{SiC}^3(1 - P_{SiC})/[P_{SiC}^2 + (1 - P_{SiC})^2]$. As a result, eq 2 leads to

$$\frac{1}{K} = \frac{1}{K_{Maxwell}} + \frac{(R_{Dia\rightarrow SiC} - R_{Dia\rightarrow Dia})}{d} \times 2P_{SiC}(1 - P_{SiC})^3/[P_{SiC}^2 + (1 - P_{SiC})^2] + \frac{R_{SiC\rightarrow Dia} - R_{SiC\rightarrow SiC}}{d} \times 2P_{SiC}^3(1 - P_{SiC}) /[P_{SiC}^2 + (1 - P_{SiC})^2] \quad (3)$$

The calculated results based on eq 3 have been plotted in Figure 1a; it can be seen that our modified model coincides with the NEMD simulation results, well-indicating that the stronger phonon scattering at the heterogeneous interfaces than that at the homogeneous interfaces is indeed the reason for the overestimation of the Maxwell model.

Although the above-calculated interface thermal resistances can reflect the stronger phonon scattering at heterogeneous interfaces, they are obtained by averaging the phonon scattering properties over the entire phonon frequencies. To understand the frequency-dependent phonon scattering at interfaces by considering contributions from phonons at different frequencies and in different branches, the interface thermal resistance R is expressed as[18]

$$R^{-1} = \frac{1}{(2\pi)^3}\int\sum_{\lambda}\hbar\omega(\boldsymbol{k}, \lambda)\frac{\partial n(\omega, T)}{\partial T}v(\boldsymbol{k}, \lambda)\alpha(\boldsymbol{k}, \lambda)\mathrm{d}\boldsymbol{k} \quad (4)$$

where $\boldsymbol{k}$ is the wave vector, λ is the phonon branch, $\hbar$ is the Planck constant, $\omega(\boldsymbol{k}, \lambda)$ is the phonon frequency with the wave vector $\boldsymbol{k}$ in branch λ, $n(\omega, T)$ is the Bose occupation factor at temperature T, $\alpha(\boldsymbol{k}, \lambda)$ is the energy transmission coefficient across the interface, and $v(\boldsymbol{k}, \lambda)$ is the phonon group velocity across the interface. Thus, it can be concluded that when the inflow of heat arises from the same material, the factors that lead to the difference between the heterogeneous and homogeneous interface thermal resistances are the transmission coefficient and the phonon group velocity across the interfaces.

To obtain the transmission coefficient and the group velocity across the interface, phonon wave packet (PWP) method[19,20] is used. In this paper, PWP simulations on phonon scattering at diamond/SiC (twist angle is 0°), diamond/diamond (twist angle is 53.13°), and SiC/SiC interfaces (twist angle is 53.13°) are carried out as examples. Figure 2a shows the snapshots of a wave packet arising from diamond scattering at diamond/SiC and diamond/diamond interfaces at different times with two instanced frequencies (1.32 and 12.92 THz). It can be seen that for the wave packet with 1.32 THz, only 4% of the incident energy is reflected at the heterogeneous interface, and nearly all incident energy can transmit across the homogeneous interface. For the wave packet with 12.92 THz, approximately 20% of the energy is reflected at the heterogeneous interface, and a significant portion of the incident energy is scattered into modes different from the incident wave packet. Approximately 10% of the energy is reflected at the homogeneous interface, and the modes of scattered energy are the same as those of the incident energy.

Figure 2b shows the frequency-dependent transmission coefficients α for wave packets comprising longitudinal acoustic (LA) phonons scattering at heterogeneous and homogeneous interfaces. It can be seen that the transmission coefficients depend strongly, but not smoothly, on the frequency of the incident wave, ω. For the wave packet arising from diamond,

DOI: 10.1021/acsomega.7b00476
ACS Omega 2017, 2, 2344−2350

the transmission coefficient at the diamond/SiC interface, $\alpha_{Dia\rightarrow SiC}$, is kept at approximately 0.96 when ω < 6 THz. Then, it decreases from 0.95 to approximately 0.5 monotonically for 6 THz < ω < 18.3 THz, and it sharply drops to zero at a frequency of 19.53 THz. Moreover, $\alpha_{Dia\rightarrow SiC}$ remains at zero for frequency ranging from 19.53 to 34.11 THz because there are no available LA modes with frequencies larger than 18.3 THz in SiC (see the inset in Figure 2b). For the diamond/diamond interface, the transmission coefficient $\alpha_{Dia\rightarrow Dia}$ is close to 1 when ω < 6 THz. Then, it decreases from 0.97 to approximately 0.75 monotonically when 6 THz < ω < 16.9 THz, and $\alpha_{Dia\rightarrow Dia}$ decreases from 0.99 to 0.235 in a fluctuation way for 16.9 THz < ω < 34.11 THz. Comparison between $\alpha_{Dia\rightarrow SiC}$ and $\alpha_{Dia\rightarrow Dia}$ shows that, with phonon frequency ranging from 1.32 to 34.11 THz, $\alpha_{Dia\rightarrow SiC}$ is lower than $\alpha_{Dia\rightarrow Dia}$ all through the considered range, making a contribution to stronger phonon scattering at diamond/SiC heterogeneous interfaces than that at diamond/diamond homogeneous interfaces. For the wave packet arising from SiC, both transmission coefficients at diamond/SiC heterogeneous and SiC/SiC homogeneous interfaces, $\alpha_{SiC\rightarrow Dia}$ and $\alpha_{SiC\rightarrow SiC}$, almost remain unchanged for ω < 5 THz. After that, a monotonic variation of transmission coefficients occurs for 5 THz < ω < 9 THz, and finally they both fluctuate for 9 THz < ω < 18.3 THz. Although the variation tendencies of $\alpha_{SiC\rightarrow Dia}$ and $\alpha_{SiC\rightarrow SiC}$ are similar, the values of $\alpha_{SiC\rightarrow Dia}$ and $\alpha_{SiC\rightarrow SiC}$ are different from each other when the frequency of the incident wave packet is the same. Note also that the value of $\alpha_{SiC\rightarrow Dia}$ is smaller than $\alpha_{SiC\rightarrow SiC}$ for ω < 9 THz, whereas $\alpha_{SiC\rightarrow Dia}$ is larger than $\alpha_{SiC\rightarrow SiC}$ for ω > 9 THz. Moreover, it can also be observed in similar cases throughout that at a low frequency (ω < 6 THz for the wave packet arising from diamond and ω < 5 THz for the wave packet arising from SiC), transmission coefficients at both heterogeneous and homogeneous interfaces are high, and they are very close to a constant, which can also be observed in other systems.[18,21] When the incident frequency is low, the phonons have a long wavelength, and they behave like classical plane waves.[22] Under this condition, the acoustic mismatch (AM) model[22] is valid, and the transmission coefficients α_{AB} between material A and material B can be obtained by

$$\alpha_{AB} = \frac{4Z_A Z_B}{(Z_A + Z_B)^2} \quad (5)$$

where $Z = \rho v$ is the acoustic impedance, ρ is the mass density, and v is the phonon group velocity. When the incident phonon frequency is low, the phonon group velocities on both sides of the homogeneous interfaces are extremely large. Despite the effect of atomic plane orientation, the group velocities at both sides of homogeneous interfaces are very close to each other. As a result, according to the AM model, the transmission coefficients calculated for homogeneous interfaces are very close to 1.[20] For the heterogeneous interface, the calculated transmission coefficient in the AM model is approximately 0.96 based on the acoustic impedance difference between diamond and SiC.[23,24] The estimation of transmission coefficients for the heterogeneous and homogeneous interfaces in eq 5 matches well with the PWP simulation results. For the wave packet with high frequency (ω > 6 THz for the wave packet arising from diamond and ω > 5 THz for the wave packet arising from SiC), a monotonically decreased tendency of transmission coefficients first occurs with increased frequencies, which results from the decreasing phonon wavelength. After that, the transmission coefficients fluctuate with increased frequency, and this phenomenon has been demonstrated to be closely related to the mismatch of phonon density of states between the grain and interface regions.[25]

Besides the energy transmission coefficient, the phonon group velocity across the interface is another factor that causes differences between the heterogeneous and homogeneous interface thermal resistances according to eq 4, and it can be reflected by the wave packet velocity across the interface. In the PWP simulation, the widths of wave packets arising from the same material across heterogeneous and homogeneous interfaces are the same (refer to Discussion 1). Thus, for wave packets with the same origin, comparison of velocities between the wave packets across heterogeneous and homogeneous interfaces can be estimated by comparing the transmission times Γ. The transmission time is the time difference between the start and the end times of wave packet energy transmission between the two sides of the interface. Figure 3a shows the start and end times for a wave packet with an instanced incident frequency 1.15 THz arising from diamond across diamond/SiC and diamond/diamond interfaces. It can

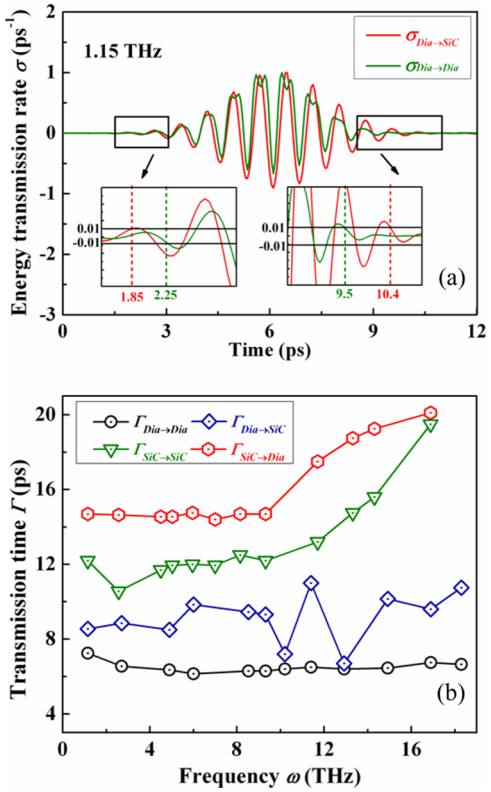

Figure 3. Comparison of transmission times for the wave packet across heterogeneous and homogeneous interfaces. (a) Start and end times of energy transmission for the wave packet arising from diamond with 1.15 THz across diamond/SiC and diamond/diamond interfaces. $\sigma_{Dia\rightarrow SiC}$ and $\sigma_{Dia\rightarrow Dia}$ are the transmission rates for the wave packet across diamond/SiC and diamond/diamond interfaces, respectively. Inset: Magnified start and end times of energy transmission for diamond/diamond and diamond/SiC interfaces. (b) Transmission times for the wave packet across heterogeneous and homogeneous interfaces. $\Gamma_{Dia\rightarrow SiC}$ and $\Gamma_{Dia\rightarrow Dia}$ are the transmission times for the wave packet arising from diamond across diamond/SiC and diamond/diamond interfaces, respectively. $\Gamma_{SiC\rightarrow Dia}$ and $\Gamma_{SiC\rightarrow SiC}$ are the transmission times for the wave packet arising from SiC across diamond/SiC and SiC/SiC interfaces, respectively.

DOI: 10.1021/acsomega.7b00476
ACS Omega 2017, 2, 2344−2350

be seen that when the wave packet goes across the diamond/SiC interface, energy transmission starts at 1.85 ps and finishes at 10.4 ps. When the wave packet goes across the diamond/diamond interface, the start and end times are 2.25 and 9.5 ps, respectively. Different start and end times for wave packet across heterogeneous and homogeneous interfaces can also be observed in some other situations, as shown in Figure S2. By calculating the time difference between the start and end times of the wave packet energy transmission, the transmission times for the wave packet across heterogeneous and homogeneous interfaces at different frequencies can be obtained. As can be seen in Figure 3b, for the wave packet arising from diamond, when the incident frequency ranges from 1.15 to 18.3 THz, the transmission time for wave packet across the diamond/SiC interface, $\Gamma_{Dia\rightarrow SiC}$, varies between 6.15 and 7.3 ps, whereas the transmission time for the diamond/diamond interface, $\Gamma_{Dia\rightarrow Dia}$, varies between 7.2 and 11 ps. Comparison between $\Gamma_{Dia\rightarrow SiC}$ and $\Gamma_{Dia\rightarrow Dia}$ indicates that when the incident frequency is the same, the value of $\Gamma_{Dia\rightarrow SiC}$ is larger than $\Gamma_{Dia\rightarrow Dia}$. Similarly, for the wave packet arising from SiC, it can also be observed that the transmission time for the wave packet across the diamond/SiC interface, $\Gamma_{SiC\rightarrow Dia}$, is larger than that across the SiC/SiC interface, $\Gamma_{SiC\rightarrow SiC}$. Thus, it can be concluded that for the wave packet with the same origin, heterogeneous interfaces prolong the energy transmission time compared with the homogeneous interfaces. This is another important reason for stronger phonon scattering at heterogeneous interfaces than that at homogeneous interfaces.

Moreover, by applying the inverse relationship between the wave packet velocity and the transmission time ($v \propto 1/\Gamma$) in eq 4, when the wave packet arises from the same material, for a certain incident frequency, the ratio between the thermal resistances of heterogeneous (R_{Heter}) and homogeneous (R_{Homo}) interfaces can be obtained by

$$\frac{R_{Heter}}{R_{Homo}} = \frac{\alpha_{Homo}(\boldsymbol{k}, \lambda)/\Gamma_{Heter}(\boldsymbol{k}, \lambda)}{\alpha_{Heter}(\boldsymbol{k}, \lambda)/\Gamma_{Homo}(\boldsymbol{k}, \lambda)} \quad (6)$$

where α_{Homo} and Γ_{Homo} are the transmission coefficient and the transmission time for the homogeneous interface and α_{Heter} and Γ_{Heter} are the transmission coefficient and the transmission time for the heterogeneous interface. Thus, the frequency-dependent R_{Heter}/R_{Homo} can be obtained by applying the transmission coefficient and transmission time in PWP simulations. As shown in Figure 4, for the wave packet arising from diamond, when the incident frequency ranges from 1.15 to 18.3 THz, the value of $R_{Dia\rightarrow SiC}/R_{Dia\rightarrow Dia}$ varies between 1.2 and 2.6, and this range includes the ratio between $R_{Dia\rightarrow SiC}$ and $R_{Dia\rightarrow Dia}$ in NEMD simulations. For the wave packet arising from SiC, when the incident frequency ranges from 1.15 to 16.9 THz, $R_{SiC\rightarrow Dia}/R_{SiC\rightarrow SiC}$ varies between 0.17 and 1.52, also including the value of $R_{SiC\rightarrow Dia}/R_{SiC\rightarrow SiC}$ in NEMD simulations. Thus, it can be concluded that when heat flow arises from the same material, stronger phonon scattering at heterogeneous interfaces than that at homogeneous interfaces is caused by the combined actions of transmission coefficients and transmission time.

CONCLUSIONS

In summary, diamond/SiC polycrystalline composites are proposed as a prototype for studying the thermal properties of heterogeneous and homogeneous interfaces. The thermal resistances of heterogeneous and homogeneous interfaces are obtained using NEMD simulations. The results indicate that when the inflow of heat arises from the same material, phonon scattering at heterogeneous interfaces is stronger than that at homogeneous interfaces. PWP simulations are carried out to analyze the different scattering mechanisms at the heterogeneous and homogeneous interfaces, and the results show that the stronger phonon scattering at heterogeneous interfaces is caused by the combined actions of energy transmission coefficients and transmission time. Our findings provide a practical guidance on how to adjust the thermal resistance of polycrystalline materials by introducing heterogeneous interfaces in polycrystalline materials.

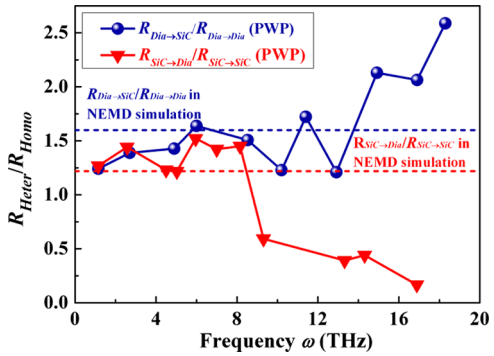

Figure 4. Frequency-dependent ratios between heterogeneous and homogeneous interface thermal resistances. $R_{Dia\rightarrow SiC}/R_{Dia\rightarrow Dia}$ is the ratio between diamond/SiC and diamond/diamond interface thermal resistances when the inflow of heat arises from diamond, and $R_{SiC\rightarrow Dia}/R_{SiC\rightarrow SiC}$ is the ratio between diamond/SiC and SiC/SiC interface thermal resistances when the inflow of heat arises from SiC.

SIMULATION SECTION

Thermal Conductivity Calculation of Diamond/SiC Polycrystalline Composites. The atomic structures of diamond/SiC polycrystalline composites are built with in-house software using the three-dimensional Voronoi tessellation method[26] (details can be found in Discussion 2). The grain sizes of composites are 2 nm, and the total number of composite grains in the simulation is 16. The diamond and SiC grains are distributed randomly in the composites, and the SiC volume fraction ranges from 0 to 100%, which is controlled by varying the number of diamond grains and SiC grains. To calculate the thermal conductivity of diamond/SiC polycrystalline composites, nonequilibrium molecular dynamics simulations are carried out (details can be found in Discussion 3). All simulations are conducted in the LAMMPS[27] package at a temperature of 300 K. Tersoff potential,[28] which has been verified accurate for thermal conductivity calculations, is used to describe C−C and Si−C bonding interactions. After energy minimization, the simulation structures are first equilibrated for 40 ps under the NPT ensemble with a constant pressure of 1 bar. After they are fully equilibrated, NEMD simulations are carried out on the relaxed structures to establish temperature gradients. Finally, thermal conductivity is calculated based on Fourier's law.[6]

Interface Thermal Resistance Calculation. To calculate the interface thermal resistance, structures of heterogeneous and homogeneous interfaces with different twist angles are created (refer to Discussion 4). To avoid the effect of sample length on the interface thermal resistance, the length of the simulation cells are chosen as 40 nm. NEMD simulations[29,30]

DOI: 10.1021/acsomega.7b00476
ACS Omega 2017, 2, 2344−2350

are performed to calculate the interface thermal resistance with a time step of 1 fs, and the temperature used is 300 K in all simulations. Tersoff potential[28] is used to describe C−C and Si−C bonding interactions. Periodic boundary conditions are applied in all three directions. Structural relaxation and temperature equilibration are first carried out with the NPT ensemble. Then, heat flux is imposed on the relaxed structures with the NVE ensemble, as shown in Figure S5a; a temperature discontinuity (ΔT) appears at the interface, as shown in Figure S5b. The interface thermal resistance R is calculated as the ratio between ΔT and the heat flux density J passing through the interface[14]

$$R = \Delta T/J \tag{7}$$

Energy Transmission Coefficients Calculation. To calculate the energy transmission coefficients, the PWP method (refer to Discussion 1) is used by implementing it in the LAMMPS package.[31] The PWPs are formed from the linear combinations of vibrational eigenstates, which are found by diagonalizing the dynamical matrix of the perfect crystal.[19] Following Schelling et al.,[19] Gaussian wave packets propagating from the left of the interface to the right are applied along the [001] direction. In PWP simulations, all wave packets are LA waves, and the length of our simulated system is 2000a (2000a diamond or SiC for homogeneous interfaces and 1000a diamond and 1000a SiC for heterogeneous interfaces) in the propagation direction. Periodic boundary conditions are applied in all three directions. Tersoff potential[28] is used to describe C−C and C−Si bonding interactions. The ambient temperature is 0 K,[20] the ensemble used is NVE, and time step is chosen as 1 fs. The energy transmission coefficient α can then be computed as

$$\alpha = \frac{E_R}{E_0} \tag{8}$$

where E_R is the transmitted energy on the right side of the interface and E_0 is the energy of the initial wave packet at time t = 0 ps.

Energy Transmission Time Calculation. To calculate the energy transmission time, the time-dependent energy transmission coefficient is calculated first, as shown in Figure S6. Then, the time-dependent transmission coefficient is differentiated with respect to time, and the energy transmission rate σ at different moments is obtained, as shown in Figure 3a. It can be seen that the transmission rate fluctuates between −1 and 1. The first moment at which the absolute value of transmission rate equals 0.01 is defined as the start time of energy transmission, and the final moment at which the absolute value of transmission rate equals 0.01 is defined as the end time of energy transmission. Energy transmission time Γ can then be obtained by calculating the time difference between the start Γ_S and end time Γ_E of energy transmission

$$\Gamma = \Gamma_E - \Gamma_S \tag{9}$$

■ ASSOCIATED CONTENT

Supporting Information

The Supporting Information is available free of charge on the ACS Publications website at DOI: 10.1021/acsomega.7b00476.

Description of PWP method, construction of diamond/SiC polycrystalline composites, nonequilibrium molecular dynamics simulations for thermal conductivity calculation, and creation of homogeneous and heterogeneous interface structures (PDF)

■ AUTHOR INFORMATION

Corresponding Author

*E-mail: wenbin@ysu.edu.cn (B.W.).

ORCID

Bin Wen: 0000-0001-9846-5452

Notes

The authors declare no competing financial interest.

■ ACKNOWLEDGMENTS

This work was supported by the National Natural Science Foundation of China under grant numbers 51372215. Y.Z. acknowledges the support from the U.S. National Science Foundation under grant number CBET-1404482. R.M. acknowledges the support from the NSERC and CRC programs, Canada.

■ REFERENCES

(1) Yang, H.-S.; Bai, G.-R.; Thompson, L. J.; Eastman, J. A. Interfacial thermal resistance in nanocrystalline yttria-stabilized zirconia. *Acta Mater.* **2002**, *50*, 2309−2317.

(2) Ni, B.; Watanabe, T.; Phillpot, S. R. Thermal transport in polyethylene and at polyethylene−diamond interfaces investigated using molecular dynamics simulation. *J. Phys.: Condens. Matter* **2009**, *21*, 084219.

(3) Millett, P. C.; Wolf, D.; Desai, T.; Rokkam, S.; El-Azab, A. Phase-field simulation of thermal conductivity in porous polycrystalline microstructures. *J. Appl. Phys.* **2008**, *104*, 033512.

(4) Meyers, M. A.; Mishra, A.; Benson, D. J. Mechanical properties of nanocrystalline materials. *Prog. Mater. Sci.* **2006**, *51*, 427−556.

(5) Nan, C.-W.; Birringer, R. Determining the Kapitza resistance and the thermal conductivity of polycrystals: A simple model. *Phys. Rev. B: Condens. Matter Mater. Phys.* **1998**, *57*, 8264.

(6) Dong, H.; Wen, B.; Melnik, R. Relative importance of grain boundaries and size effects in thermal conductivity of nanocrystalline materials. *Sci. Rep.* **2014**, *4*, 7037.

(7) Li, Q.; Liu, C.; Fan, S. Thermal boundary resistances of carbon nanotubes in contact with metals and polymers. *Nano Lett.* **2009**, *9*, 3805−3809.

(8) Hasselman, D. P. H.; Donaldson, K. Y.; Liu, J.; Gauckler, L. J.; Ownby, P. D. Thermal Conductivity of a Particulate-Diamond-Reinforced Cordierite Matrix Composite. *J. Am. Ceram. Soc.* **1994**, *77*, 1757−1760.

(9) Jiajun, W.; Xiao-Su, Y. Effects of interfacial thermal barrier resistance and particle shape and size on the thermal conductivity of AlN/PI composites. *Compos. Sci. Technol.* **2004**, *64*, 1623−1628.

(10) Kim, H. S.; Jang, J.-u.; Yu, J.; Kim, S. Y. Thermal conductivity of polymer composites based on the length of multi-walled carbon nanotubes. *Composites, Part B* **2015**, *79*, 505−512.

(11) Gong, F.; Bui, K.; Papavassiliou, D. V.; Duong, H. M. Thermal transport phenomena and limitations in heterogeneous polymer composites containing carbon nanotubes and inorganic nanoparticles. *Carbon* **2014**, *78*, 305−316.

(12) Zhang, W.; Fisher, T. S.; Mingo, N. Simulation of Interfacial Phonon Transport in Si−Ge Heterostructures Using an Atomistic Green's Function Method. *J. Heat Transfer* **2007**, *129*, 483.

(13) Chen, Y.; Li, D.; Yang, J.; Wu, Y.; Lukes, J. R.; Majumdar, A. Molecular dynamics study of the lattice thermal conductivity of Kr/Ar superlattice nanowires. *Phys. B* **2004**, *349*, 270−280.

(14) Crocombette, J. P.; Gelebart, L. Multiscale modeling of the thermal conductivity of polycrystalline silicon carbide. *J. Appl. Phys.* **2009**, *106*, 083520.

(15) Kidalov, S. V.; Shakhov, F. M. Thermal Conductivity of Diamond Composites. *Materials* **2009**, *2*, 2467−2495.

DOI: 10.1021/acsomega.7b00476
ACS Omega 2017, 2, 2344−2350

(16) Pei, Q.-X.; Zhang, Y.-W.; Sha, Z.-D.; Shenoy, V. B. Carbon isotope doping induced interfacial thermal resistance and thermal rectification in graphene. *Appl. Phys. Lett.* **2012**, *100*, 101901.
(17) Hahn, K. R.; Puligheddu, M.; Colombo, L. Thermal boundary resistance at Si/Ge interfaces determined by approach-to-equilibrium molecular dynamics simulations. *Phys. Rev. B: Condens. Matter Mater. Phys.* **2015**, *91*, 195313.
(18) Zhao, H.; Freund, J. B. Lattice-dynamical calculation of phonon scattering at ideal Si−Ge interfaces. *J. Appl. Phys.* **2005**, *97*, 024903.
(19) Schelling, P. K.; Phillpot, S. R.; Keblinski, P. Phonon wave-packet dynamics at semiconductor interfaces by molecular-dynamics simulation. *Appl. Phys. Lett.* **2002**, *80*, 2484−2486.
(20) Schelling, P. K.; Phillpot, S. R.; Keblinski, P. Kapitza conductance and phonon scattering at grain boundaries by simulation. *J. Appl. Phys.* **2004**, *95*, 6082−6091.
(21) Gu, X.; Li, X.; Yang, R. Phonon transmission across Mg_2Si/$Mg_2Si_{1-x}Sn_x$ interfaces: A first-principles-based atomistic Green's function study. *Phys. Rev. B: Condens. Matter Mater. Phys.* **2015**, *91*, 205313.
(22) Sun, L.; Murthy, J. Y. Molecular Dynamics Simulation of Phonon Scattering at Silicon/Germanium Interfaces. *J. Heat Transfer* **2010**, *132*, 102403.
(23) Wang, S.-F.; Hsu, Y.-F.; Pu, J.-C.; Sung, J. C.; Hwa, L. G. Determination of acoustic wave velocities and elastic properties for diamond and other hard materials. *Mater. Chem. Phys.* **2004**, *85*, 432−437.
(24) He, H.; Sekine, T.; Kobayashi, T. Direct transformation of cubic diamond to hexagonal diamond. *Appl. Phys. Lett.* **2002**, *81*, 610−612.
(25) Zheng, Z.; Chen, X.; Deng, B.; Chernatynskiy, A.; Yang, S.; Xiong, L.; Chen, Y. Phonon thermal transport through tilt grain boundaries in strontium titanate. *J. Appl. Phys.* **2014**, *116*, 073706.
(26) Ju, S.; Liang, X.; Xu, X. Out-of-plane thermal conductivity of polycrystalline silicon nanofilm by molecular dynamics simulation. *J. Appl. Phys.* **2011**, *110*, 054318.
(27) Plimpton, S. Fast Parallel Algorithms for Short-Range Molecular Dynamics. *J. Chem. Phys.* **1995**, *117*, 1−19.
(28) Chen, J.; Walther, J. H.; Koumoutsakos, P. Covalently Bonded Graphene-Carbon Nanotube Hybrid for High-Performance Thermal Interfaces. *Adv. Funct. Mater.* **2015**, *25*, 7539−7545.
(29) Oligschleger, C.; Schön, J. C. Simulation of thermal conductivity and heat transport in solids. *Phys. Rev. B: Condens. Matter Mater. Phys.* **1999**, *59*, 4125.
(30) Müller-Plathe, F. A simple nonequilibrium molecular dynamics method for calculating the thermal conductivity. *J. Chem. Phys.* **1997**, *106*, 6082.
(31) Ju, S.-H.; Liang, X.-G. Investigation on interfacial thermal resistance and phonon scattering at twist boundary of silicon. *J. Appl. Phys.* **2013**, *113*, 053513.

DOI: 10.1021/acsomega.7b00476
ACS Omega 2017, 2, 2344−2350